Pd(II)-doping studies on tris(thiourea)zinc(II) sulphate crystals: Catalytic effect of Pd(II)-doping on SHG efficiency

M Rajasekar[a,b], G Ramasamy[a] & S P Meenakshisundaram[a]*

[a]Department of Chemistry, Annamalai University, Annamalainagar 608 002, India
[b]K S R College of Engineering, K S R Kalvinagar, Tiruchengode 637 215, India

Single crystals of Pd(II)-doped tris(thiourea)zinc(II) sulphate (ZTS) have been grown from an aqueous solution by conventional slow evaporation solution growth technique. The characteristic functional groups have been identified by FTIR analysis. Crystal stress has been indicated by powder XRD patterns and FTIR analysis. Incorporation of dopant into the crystalline matrix during crystallization process has been evidenced by energy dispersive X-ray spectroscopy and quantified by inductively coupled plasma technique. The surface morphological changes have been observed in the doped specimen. Mechanical stability of the as-grown specimen has been analyzed by Vickers microhardness analysis. Thermal studies reveal no decomposition up to the melting point. Lattice parameters determined by single crystal XRD analysis reveal only minor variations as a result of low doping. Pd(II) doping has a catalytic effect on the second harmonic generation efficiency improvement of zinc thiourea complex.

Keywords: Crystal growth, Optical properties, Mechanical properties, TG/DTA, Nonlinear optics

1 Introduction

Tris(thiourea)zinc(II) sulphate is a semi-organic nonlinear optical material which finds applications in the area of laser technology, optical communication, data storage and optical computing because it has a high resistance to laser induced damage, high nonlinearity, wide transparency, low angular sensitivity and good mechanical hardness compared to many organic NLO crystals[1-4]. ZTS is a good engineering material for second harmonic generation (SHG) device applications. It is a novel metal organic crystal with potential application in electo-optic modulation[5]. It crystallizes in orthorhombic system with noncentrosymmetric space group Pca2₁ (point group mm2). Metal ion doped materials are currently receiving a great deal of attention due to the rapid development of laser diodes[6,7]. Transition metal impurity in the crystalline matrix generally influences the physical properties of the crystal[8-13]. Palladium doping enhances the gas sensing properties of nanoparticles[14-19]. Incorporation of palladium strongly affects the manganese reducibility and shifts the reduction process to lower temperature[20]. Also, palladium doping enhances the stability of gold cluster[21]. In the present investigation, Pd(II)- doping

effects on thiourea complex has been reported, particularly in the improvement of SHG-activity.

2 Experimental Details

2.1 Synthesis and crystal growth

ZTS was synthesized[22] using zinc sulphate heptahydrate (EM) and thiourea (SQ) in a stoichiometric ratio of 1:3. To avoid decomposition, low temperature (<70 °C) was maintained during the preparation of solution in deionized water.

$$ZnSO_4.7H_2O + 3(CS(NH_2)_2) \rightarrow Zn(CS(NH_2)_2)_3SO_4$$
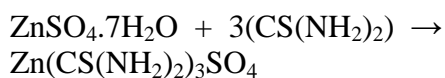
After successive recrystallization processes, crystals were grown by slow evaporation solution growth technique[23,24]. Doping of palladium (5 mol%) in the form of palladium chloride was done during the crystallization process. The crystallization took place in 20-23 days and the macroscopic defect-free crystals were harvested. Photographs of as-grown pure and palladium(II) doped ZTS crystals are shown in Fig. 1.

2.2 Characterization studies

The FTIR spectra were recorded by using AVATAR 330 FTIR spectrometer using the KBr pellet technique in the range of 400-4000 cm⁻¹. The powder XRD data were analyzed with the PAN
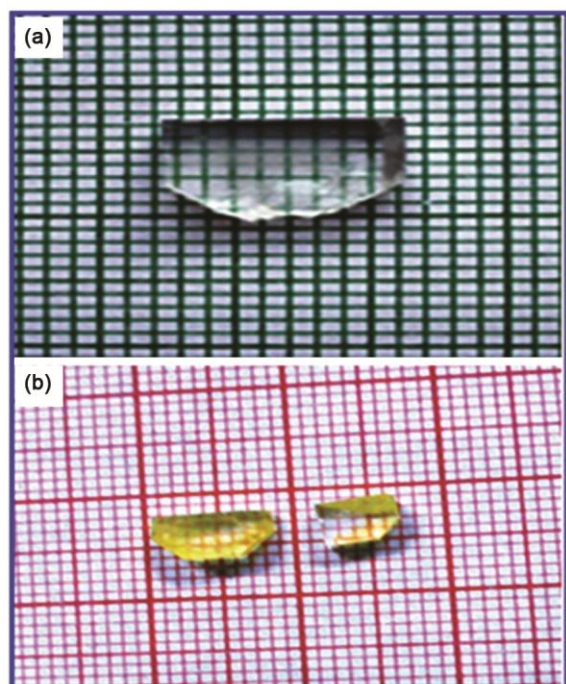
Fig. 1 — Photographs of as-grown ZTS crystals (a) pure and (b) Pd(II)- doped

Fig. 2 — FTIR spectra of ZTS

Table 1 — FTIR characteristic vibrational frequencies

S. No.	Thiourea	ZTS	Pd(II)- doped ZTS	Assignment of vibrations
1	3376	3399	3406	$\nu_{as}(NH_2)$
2	3167	3195	3196	$\nu_s(NH_2)$
3	1627	1624	1626	$\delta(NH_2)$
4	1089	1122	1157	$\nu_s(C\text{-}N)$
5	1472	1502	1505	$\nu(N\text{-}C\text{-}N)$
6	1417	1398	1430	$\nu_{as}(C=S)$
7	740	712	713	$\nu_s(C=S)$
8	648	619	619	$\nu_{as}(N\text{-}C\text{-}S)$
9	492	471	476	$\delta_{as}(N\text{-}C\text{-}N)$

analytical model- X'pert PRO analyzer using graphite monochromated Cu-Kα radiation. The Vickers microhardness measurement was done using a Reichert 4000E Ultramicrohardness tester. CARY 5E UV- visible spectrometer was used for the UV-visible studies. DTA curves were recorded on a SDT Q 600 (TA instrument) thermal analyzer using nitrogen atmosphere. The SHG of the specimens were measured by the Kurtz powder technique[25]. An Nd:YAG laser with modulated radiation of 1064 nm was the optical source. Uniform particle size (125-150 μm) specimens were exposed to laser and the output was monochromated to collect the intensity of the 532 nm component. The surface morphologies of the samples were observed using a JEOL JSM 5610 LV scanning electron microscope which has a resolution of 3.0 nm and an acceleration voltage of 0.3-20 kV having the maximum magnification of 2,00,000 times. The ICP studies were recorded on optima 5000 DV series spectrometer. The single crystal X-ray diffraction analysis was done using Bruker Axis (Kappa APEXII) X-ray diffractometer with Mo K$_\alpha$ radiation to determine the cell parameters.

3 Results and Discussion

3.1 FTIR studies

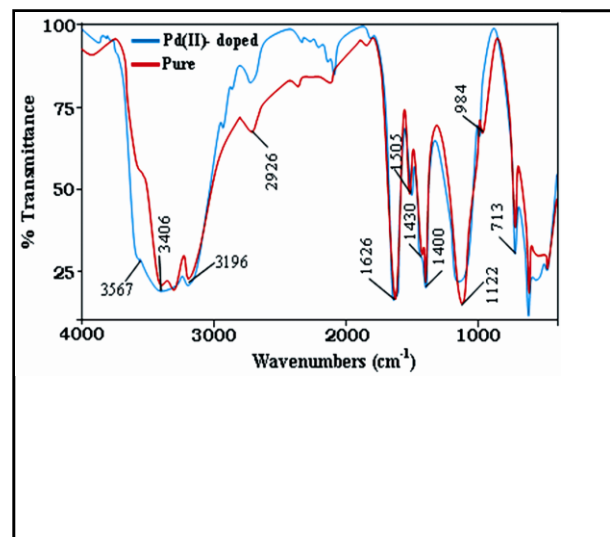A close observation of FTIR spectra (Fig. 2) of the pure and doped specimens reveals that the doping results in small shifts in some of the characteristic vibrational frequencies (Table 1). The CN stretching frequencies of thiourea (1089 cm^{-1} and 1472 cm^{-1}) are shifted to higher frequencies for Pd(II) doped ZTS (1157 cm^{-1} and 1505 cm^{-1}). The CS stretching frequencies (1417 cm^{-1} and 740 cm^{-1}) are shifted to lower frequencies (1430 cm^{-1} and 713 cm^{-1}) for doped specimens. An absorption band in the region 2750 to 3400 cm^{-1} corresponds to the symmetric and asymmetric stretching frequencies of NH$_2$ group of zinc (II) coordinated thiourea. Spectral studies suggest that the metal coordinate with thiourea through sulfur atom. The minor changes in the vibrational patterns could be associated with the crystal stress developed as a result of dopant incorporation.

3.2 XRD studies

A comparison of powder XRD patterns of pure and doped Pd(II) specimens reveals the intensity variations (Fig. 3). Diffraction patterns indicate no phase changes and narrow peaks indicate good crystallinity.
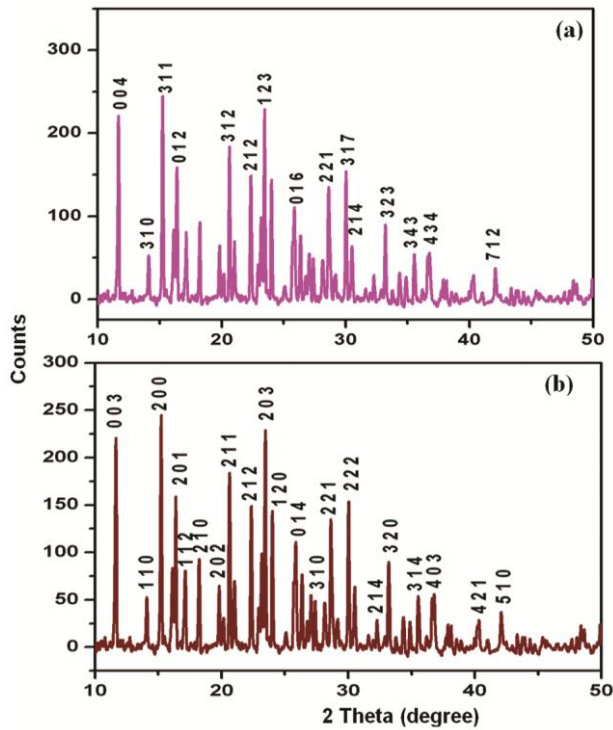
Fig. 3 — Powder XRD patterns of ZTS (a) pure and (b) Pd(II)-doped

Table 2 – Lattice parameters

System	a (Å)	b (Å)	c (Å)	Volume (Å^3)
Pure ZTS*	11.21	7.72	15.6	1350.23
Pd(II)- doped ZTS	7.80	11.32	15.51	1369

*JCPDS no: 76-0778

However, a slight variation in intensity is observed as a result of doping. The most prominent peaks with maximum intensity of the XRD patterns of pure and doped specimens are quite different. These observations could be attributed to the strains in the lattice, developed due to doping. The cell parameters are determined from the single crystal X-ray diffraction analysis (Table 2) and the as-grown crystal belongs to the monoclinic system. Minor variations in cell parameters are justified because of low doping levels.

3.3 SEM and EDS/ICP

The effect of the influence of dopant on the surface morphology of ZTS crystal faces reveals structure defect centers and voids as seen in the SEM micrographs (Fig. 4). The micrographs of the doped specimen show more scatter centers than that of the undoped specimen. A small quantity incorporation of Pd(II)- in the doped specimen was confirmed by EDS as clearly seen in Fig. 5.

Palladium incorporation is clearly revealed by inductively coupled plasma (ICP) technique; the incorporation (1.2 ppm) is small but significant. The dopant concentration in the host lattice is not proportional to the concentration taken during the crystallization process since the host crystal can accommodate the dopant only to a limited extent. Ease of incorporation even by small quantity doping is justified by comparing the ionic radii of Zn^{2+} (74 ppm) with that of Pd^{2+} (78 ppm).

3.4 UV-visible spectra

A comparison of UV-Vis spectra of pure and undoped ZTS (Fig. 6) clearly reveals that the transmittance range is extended in the visible region, a required property for an NLO material and it could be used for optical window applications. The lower cut-off wavelength is ~300 nm. The band gap energy of the specimen is estimated as 4.68 eV for doped specimen by diffuse reflectance spectral data, using Tauc plot, $[F(R) \, hv]^{1/2}$ vs hv (eV) where hv is the photon energy and $F(R)$ is the Kubelka-Munk function obtained from reflectance data[26].
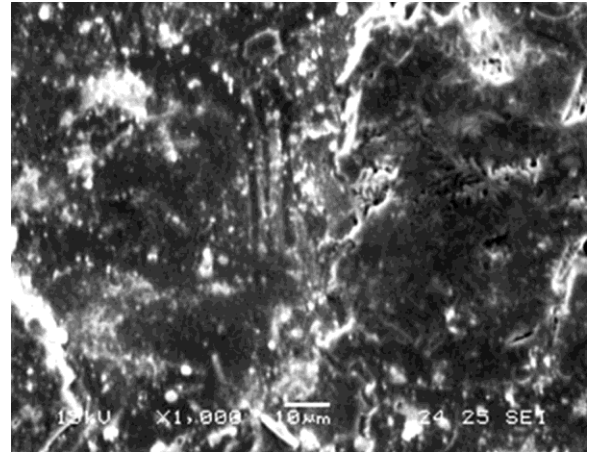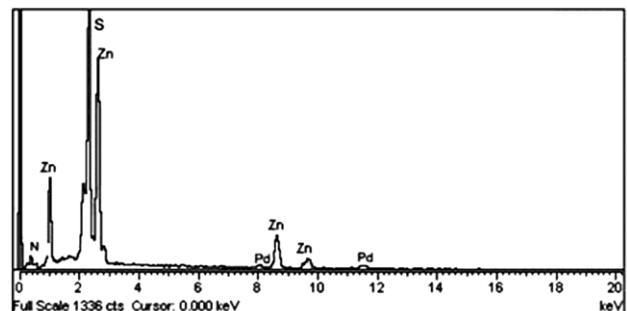

Fig. 4 — SEM micrographs of Pd(II)- doped ZTS

Fig. 5 — EDS spectrum of Pd(II)- doped ZTS

3.5 Thermal studies

The simultaneous TG/DTA curves in nitrogen recorded for doped ZTS specimen are given in Fig. 7. The absence of water of crystallization in the molecular structure is indicated by the absence of weight loss around 100 ºC. The melting point of sample is slightly decreased in the case of Pd(II) doped ZTS suggesting the incorporation. No decomposition up to the melting point ensures the suitability of the material for the application in lasers where the crystals are required to withstand high temperatures.

3.6 Mechanical studies

Transparent crystals free from cracks were selected for microhardness measurements. Before indentation, the crystals were carefully lapped and washed to avoid surface effects. The Vickers hardness indentations were made on the as-grown surface of the Pd(II)- doped crystal at room temperature with the load ranging from 25 to 100 g, keeping the time of indentations kept as 10 s for all trials. The Vickers hardness number (H_v) was calculated using the relation:

$$H_v = 1.8544(P/d^2) \text{ kg/mm}^2$$

where P is the applied load in kg and d is the mean diagonal length of the indentation impression in micrometer. A plot of Vickers hardness number (H_v) versus load (P) reveals that the hardness of the grown crystal increases as the load increases (Fig. 8). Cracks started developing around the indentation mark beyond a load of 100 g. This may be due to the internal stresses released during the indentation. The hardness of the material is found to increase with the increase of load confirming the prediction of Onitsch[27] and the work hardening index is equal to 3.53.

3.7 SHG efficiency

An Nd:YAG laser with modulated radiation of 1064 nm was the optical source. Uniform particle size (125-150 μm) specimens were exposed to laser (Input energy-2.5 mJ/pulse) and the output was monochromated to collect the intensity of the 532 nm component. In order to confirm the influence of doping on the SHG-activity and as a comparative measure, the pure and Pd(II)- doped specimens were subjected to SHG test. The output SHG intensities give the relative efficiencies of the measured specimens and the effect of various metal dopants on the SHG efficiency of ZTS has been listed in Table 3. From this data, it is clear that the metal doping enhances the SHG efficiency. Metals can behave as electron donors or acceptors and it appears that they facilitate the charge transfer thereby nonlinearity. A favorable molecular alignment for nonlinearity is
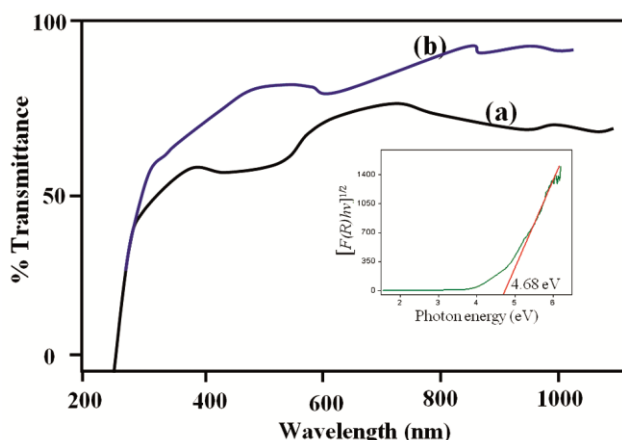
Fig. 6 — UV-visible spectra of ZTS specimens (a) pure and (b) Pd(II)- doped
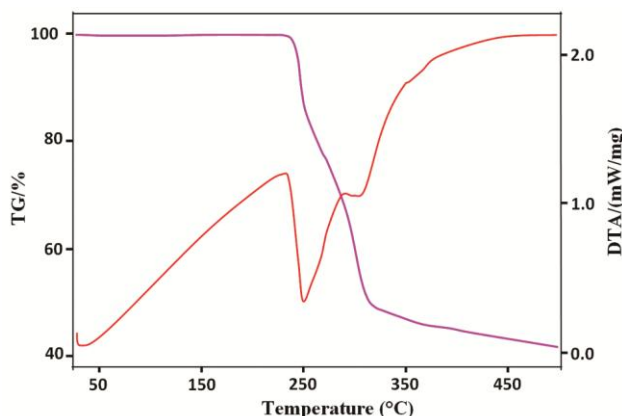
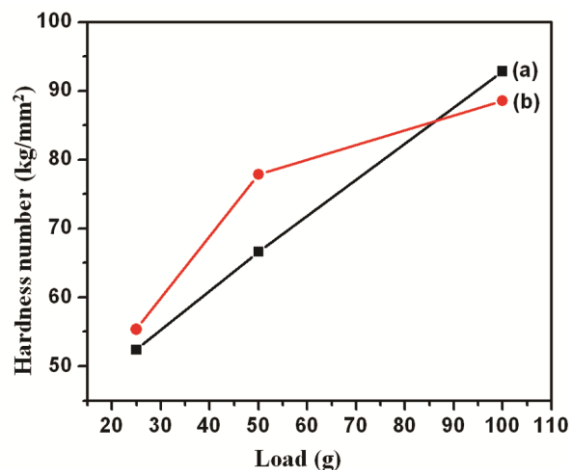Fig. 7 — TG-DTA curves of Pd(II)- doped ZTS

Fig. 8 — Plot of Vickers hardness number vs load (a) pure and (b) Pd(II)- doped ZTS

Table 3 – SHG outputs of metal doped ZTS

System	Relative efficiency	Reference
ZTS doped Pd(II)	~1.7 times of ZTS	Present Work
ZTS doped with Ce(IV)	~ 1.6 times of ZTS	24
ZTS doped with Mn(II)	~ 2.1 times of ZTS	28
ZTS doped with Cs(I)	~1.2 times of ZTS	29
ZTS doped with K(I)	~ 1.2 times of KDP	30,31
ZTS doped with Na(I)	Slightly greater than ZTS	32
ZTS doped with Li(I)	Green light emission	33
ZTS doped with Cd(II)	Greater than ZTS	34
ZTS doped with Ni(II)	~1.4 times of ZTS	35

achieved by incorporation of small quantity of metal into the crystalline matrix. It is interesting to observe that a small quantity incorporation of Pd(II) has a catalytic effect on SHG efficiency of ZTS.

4 Conclusions

Pd(II) extends the transmittance range of tris(thiourea)zinc(II) sulphate in the visible region. A close observation of XRD and FTIR profiles of doped specimen reveals some minor structural variations. Small quantity incorporation of foreign metal ion develops scatter centers and crystal stress. Transition metal can act as an electron donor or acceptor and Pd doping is advantageous since it improves the SHG efficiency of the host crystal to an appreciable extent. Its catalytic activity in enhancing the second harmonic generation efficiency of zinc thiourea complex is the highlight of the study and hence, Pd(II) is a useful dopant. Thermal analysis reveals that the crystal is stable up to the melting point. The doped specimen looks like a promising material for the device fabrication and can be well used in microelectronic industry.

References

1 Gupta S S & Desai C F, *Cryst Res Technol*, 34 (1999) 1329.
2 Ramabadran U B, Zelmon D E & Kennedy G C, *Appl Phys Lett*, 60 (1992) 2589.
3 Sastry P U, *Solid State Commun*, 109 (1999) 595.
4 Venkataramanan V, Dhanaraj G, Wadhawan V K, Sherwood J N & Bhat H L, *J Cryst Growth*, 154 (1995) 92.
5 Rockwell International Corporation, Seal beach, CA, Patent-US5581010: *Semi-Organic Crystals for Nonlinear Optical Devices*.
6 Long X, Wang G & Han T P J, *J Cryst Growth*, 249 (2003) 191.
7 Ramajothi J & Dhanuskodi S, *Cryst Res Technol*, 38 (2003) 986.
8 Camargo M B, Stultz R D, Birnbaum M & Kokta M, *Opt Lett*, 20 (1995) 339.
9 Denisov I A, Demchuk M L, Kuleshov N V & Yumashec K V, *Appl Phys Lett*, 77 (2000) 2455.
10 Duan X L, Yuan D R, Wang L H, Yu F P, Cheng X F, Liu Z Q & Yan S S, *J Cryst Growth*, 296 (2006) 234.
11 Kuleshov N V, Mikhailov V P, Scherbitsky V G, Prokoshin P V & Yumashev K V, *J Lumin*, 55 (1993) 265.
12 Mao X, Xu F, Tang J, Gao W, Li S & Du Y, *J Magn Magn Mater*, 288 (2005) 106.
13 Yumashev K V, *Appl Opt*, 38 (1999) 6343.
14 Rui-Qin T, Yan-Qu G, Jun-Hua Z, Yue L, Tie-Feng X & Wei-Jie S, *Trans Nonferrous Met Soc China,* 21 (2011) 1568.
15 Al-Zaidi Q G, Suhail A M & Al-Azawi W R, *Appl Phys Res*, 3 (1) (2011) 89.
16 Aquila K D, Dravid V, Donthu S & Pan Z, *Nanoscale*, 5 (1) (2008) 85.
17 Erades L, Grandjean D, Nayral C, Soulantica K, Chaudret B, Menini P, Parret F & Maisonnat A, *New J Chem,* 30 (2006) 1026.
18 Liang H H & Lee J Y, *Enhanced electro-optical properties of liquid crystals devices by doping with ferroelectric nanoparticles*, Department of Materials Science and Engineering, University of Science and Technology, Taiwan. (InTech), 2011.
19 Gallego N C, Contescu C I, Bhat V V, Benthem K V, Tekinalp H & Edie D D, *Palladium-doped nonoporous carbon fibers for hydrogen storage,* International conference on carbon, CARBON 2008, Nagano, Japan, 2008.
20 Baylet A, Royer S, Labrugere C, Valencia H, Marecot P, Tatibouet J M & Duprez D, *Phys Chem Chem Phys*, 10 (2008) 5983.
21 Mushrif S H, Rey A D & Peslherbe G H, *J Mater Chem*, 20 (2010) 6859.
22 Ushasree P M, Muralidharan R, Jayavel R & Ramasamy P, *J Cryst Growth*, 210 (2000) 741.
23 Meenakshisundaram S, Parthiban S, Sarathi N, Kalavathy R & Bhagavannarayana G, *J Cryst Growth*, 293 (2006) 376.
24 Kasturi L, Bhagavannarayana G, Parthiban S, Ramasamy G, Muthu K & Meenaksisundaram S, *Cryst Eng Commun*, 12 (2010) 493.
25 Kurtz S K & Perry J J, *J Appl Phys*, 39 (1968) 3798.
26 Karunakaran C, Abiramasundari G, Gomathisankar P, Manikandan G & Anandi V, *J Coll Inter Sci*, 352 (2010) 68.
27 Onitsch E M, *Mikroskopie,* 2 (1947) 131.
28 Bhagavannarayana G, Kushwaha S K, Parthiban S & Meenakshisundaram S, *J Cryst Growth*, 311 (2009) 960.
29 Muthu K & Meenakshisundaram S P, *J Phys Chem Solids*, 73 (2012) 1146.
30 Krishnan C, Selvarajan P & Freeda T H, *J Cryst Growth*, 311 (2008)141.
31 Krishnan C, Selvarajan P & Freeda T H, *Mater Lett*, 62 (2008) 4414.
32 Krishnan C, Selvarajan P & Pari S, *Curr Appl Phys*, 10 (2010) 664.
33 Krishnan C, Selvarajan P & Freeda T H, *Mater Manuf Process*, 23 (2008) 800.
34 Gopinath S, Palanivel R & Rajasekaran R, *Int J Pure Appl Sci Technol*, 1 (2) (2010) 104.
35 Rajasekar M, Muthu K, Meenatchi V, Mahadevan C K & Meenakshisundaram S P, *Optik*, 125 (2014) 710.